Apical accumulation of the *Drosophila* PDGF/VEGF receptor ligands provides a mechanism for triggering localized actin polymerization

Dalia Rosin, Eyal Schejter, Talila Volk and Ben-Zion Shilo*

Department of Molecular Genetics, Weizmann Institute of Science, Rehovot 76100, Israel
*Author for correspondence (e-mail: benny.shilo@weizmann.ac.il)

Accepted 14 January 2004

Development 131, 1939-1948
Published by The Company of Biologists 2004
doi:10.1242/dev.01101

Summary

Epithelial tissue functions depend largely on a polarized organization of the individual cells. We examined the roles of the *Drosophila* PDGF/VEGF receptor (PVR) in polarized epithelial cells, with specific emphasis on the wing disc epithelium. Although the receptor is broadly distributed in this tissue, two of its ligands, PVF1 and PVF3 are specifically deposited within the apical extracellular space, implying that polarized apical activation of the receptor takes place. The apical localization of the ligands involves a specialized secretion pathway. Clones for null alleles of *Pvr* or expression of RNAi constructs showed no phenotypes in the wing disc or pupal wing, suggesting that *Pvr* plays a redundant role in this tissue. However, when uniform expression of a constitutively dimerizing receptor was induced, loss of epithelial polarity, formation of multiple adherens and septate junctions, and tumorous growth were observed in the wing disc. Elevation of the level of full-length PVR also gave rise to prominent phenotypes, characterized by higher levels of actin microfilaments at the basolateral areas of the cells and irregular folding of the tissue. Together, these results suggest that polarized PVR activation is necessary for the proper organization of the wing disc epithelium, by regulating the apical assembly of the actin cytoskeleton.

Key words: *Drosophila*, PVR, PVF, VEGF, PDGF, Epithelial polarity, Wing epithelium, Actin organization

Introduction

Epithelial tissue functions depend largely on a polarized organization of the individual cells. The characteristic cell of a simple monolayered epithelium is polarized along an apicobasal axis, in that its plasma membrane is separated into functionally distinct apical and basolateral domains (Drubin and Nelson, 1996). The apical membrane domain communicates to neighboring cells via membrane proteins, such as cell-adhesion molecules and other cell-surface receptors. These cell-adhesion molecules are often organized in large specialized multi-protein complexes forming different cell junctions (Borrmann et al., 2000; Nagafuchi, 2001). In invertebrates, epithelial junctional complexes are composed of two types of junctions, the adherens junctions and the septate junctions (Muller, 2000; Tepass et al., 2001).

Among the molecular components of adherens junctions, cadherins and catenins comprise the core of an adhesive interaction that connects subapical actin belts of adjacent cells with each other (Tepass, 2002). This association with the cytoskeletal network is necessary for stable cell-cell adhesion and for the integration of these contacts with the morphology of epithelial cells. Several signaling pathways that are activated by cell adhesion have been identified, most notably those regulated by small Rho-like GTPases (Braga, 2002). However, the molecular mechanisms governing the interactions between adherens junction components and the actin cytoskeleton remain largely unresolved issues.

Septate junctions are maintained by localization of intracellular PDZ domain proteins such as Discs large (DLG) and Scribble. In combination with their ability to multimerize, PDZ proteins have the potential to assemble large multiprotein complexes at the cell membrane (Bilder, 2001).

The generation and maintenance of polarity in epithelial cells is intimately linked to the polarized distribution of transmembrane and secreted proteins. The junctions between cells form a barrier not only to diffusion of extracellular molecules between the cells, but also to movement of molecules within the plasma membrane. Thus, in order to localize a transmembrane protein to a particular cellular compartment (apical or basolateral), it must be targeted to secretory vesicles that will specifically fuse with that membrane compartment (Mostov and Cardone, 1995; Simons and Ikonen, 1997; Wandinger-Ness et al., 1990).

In this study, we identify broad expression of the *Drosophila* PDGF/VEGF receptor (PVR) in epithelial tissues. We specifically examined possible roles of the PVR pathway in the wing disc epithelium. Two of the PVR ligands, PVF1 and PVF3, are deposited within the apical extracellular space, suggesting that polarized apical activation of the receptor may take place. Clones for null alleles of *Pvr* showed no phenotypes in the wing disc or pupal wing. However, when uniform activation of PVR was induced by a constitutively dimerizing receptor, loss of epithelial polarity, uniform appearance of adherens junctions and tumorous growth were observed in the wing disc. Elevation of full-length PVR levels also gave rise to prominent phenotypes, characterized by significantly higher levels of F-actin in the basolateral area of the epithelium. Taken together these results point to the importance of polarized

apical PVR activation in maintenance of the wing disc monolayered epithelium, via regulation of localized actin microfilament polymerization.

Materials and methods

DNA constructs

The full-length *Pvr* construct was generated by combining the signal-peptide encoding region from EST SD02385 to the remaining *Pvr*-coding region encoded by EST SD03187, to generate a full length, intronless transcript. After verification of an intact ORF, the coding region was cloned into pUAST. To generate the *UAS-dsRNA-Pvr* construct, a cDNA fragment containing bases 825-2403 in an antisense orientation (numbers correspond to bases after the initiator ATG), followed by bases 1277-2403 (sense orientation) were inserted into pUAST. The RNA transcribed from this construct should thus generate a stem of 1126 and a loop of 452 bases. Transgenic flies were generated from each construct. *pUAST-Pvf1* was generated from EST LD28763, including its 5′ and 3′ non-coding regions. *pUAST-Pvf3* was generated by PCR amplification of the full ORF of the Vegf 27Ca cDNA plasmid (GenBank Accession Number AY079183) provided by Exelixis. *pUAS-sGFP* was generated by fusing the Spitz signal peptide to EGFP.

Fly strains

The following *Gal4* driver lines were used to express the various transgenic constructs: *69B-Gal4* (expressed uniformly in the embryonic ectoderm), *actin-Gal4* (expressed ubiquitously), *MS1096-Gal4* (expressed in the pouch of the wing imaginal disc), *patched-Gal4* and *dpp-Gal4* (expressed along the anterior-posterior border of the wing disc), *GMR-Gal4* (expressed in differentiating photoreceptor cells), and *eyeless-Gal4* (expressed in all eye precursor cells). For generation of *Pvf1* 'flip out' clones the *pUAST-Pvf1* line was crossed to a line containing *hs-flp*, *UAS-GFP* and *actin>CD2>Gal4*. To generate larval clones, a 30-minute heat shock at 37°C was applied at 72-96 hours AEL. Flies containing *λPvr* were obtained from P. Rorth.

The *Pvr* mutant $Vegfr^{C2195}$ [obtained from Exelixis (Cho et al., 2002)] was recombined with *FRT 40A*. Clones were generated following a cross to *hs-flp; FRT 40A, ubi-GFP* (Bloomington #5629) or *hs-flp; FRT 40A*, *arm-lacZ* (Bloomington #6579). Three heat shocks of 1.5 hours each at 37°C were applied, starting at 24-48 hours AEL, at 24 hour intervals.

Antibodies

EST SD02385 was used to insert the region encoding PVR C-terminal residues 1291-1509 into pRSETB. Recombinant protein was purified on a NINTA column, and injected into rats. Typically, the antibody is diluted 1/200 for immunohistochemical staining. EST LD28763 was used to insert the region encoding PVF1 residues 27-303 into pRSETA. Recombinant protein was injected into rats. The antibody is diluted 1/100 for staining. To generate antibodies recognizing PVF3, PCR amplification of the region encoding residues 22-359 was carried out. The template used was Vegf 27Ca cDNA. The fragment was cloned into pRSETA. The purified recombinant protein was injected into guinea pigs, and the antibody used at a dilution of 1/100 for staining.

Rabbit anti-DLG was obtained from P. Bryant, mouse anti-LGL antibodies were obtained from F. Matsuzaki, Profilin antibodies (chi1J) from the Developmental Studies Hybridoma bank, TRITC-labeled phalloidin was purchased from Sigma, and Alexa 488 phalloidin and fluorescein conjugate deoxyribonuclease I from Molecular Probes. Monoclonal anti-GFP antibodies were obtained from Roche, and diluted 1/10 for staining, and rabbit anti-beta galactosidase from Cappel (diluted 1/1000). Secondary antibodies were obtained from Jackson ImmunoResearch, and diluted at 1/300 for staining.

Staining and microscopy

Antibody staining of wing discs was according to Neumann and Cohen (Neumann and Cohen, 1997). Staining of extracellular distribution of PVF1 and PVF3 was as described previously (Strigini and Cohen, 2000). For extracellular staining, antibodies were used at a dilution of 1/30 for PVF1 or PVF3, and 1/3 for anti-GFP. Incubation with these antibodies was carried out on ice, to block endocytosis. Staining of pupal wings was as described previously (Fristrom et al., 1994) with the following modifications: Pupal discs were fixed at 4°C for 48 hours, and mounted in Aquamount after staining.

For sections, wing discs were fixed in 4% glutaraldehyde and 4% formaldehyde, embedded in JB4 (Polysciences), and stained in Hematoxylin and Eosin after sectioning.

For EM, discs were fixed by immersion in freshly prepared 3% paraformaldehyde, 2% glutaraldehyde in cacodylate buffer containing 5 mM $CaCl_2$ (pH 7.4) for 2 hours at room temperature and for 12 hours at 4°C. After washing, the tissue was post fixed in osmium tetroxide, 0.5% potassium dichromate and 0.5% potassium hexacyanoferrate in cacodylate buffer for 1 hour. The tissue was stained and blocked with 2% aqueous uranyl acetate followed by ethanol dehydration. The samples were embedded in EMBED 812. Thin sections were cut using a diamond knife, stained with 2% uranyl acetate and Reynolds's lead citrate, and examined with a transmission electron microscope (Philips, CM12) at an accelerating voltage of 120 kV.

Heparin binding assay

Schneider S2 cells were transiently transfected with actin-Gal4 and pUAST-PVF1 or pUAST-sGFP plasmids, and grown in serum-free medium for 3 days. Medium was collected and incubated for 3 hours with Heparin-Sepharose cl-6B beads (Pharmacia). Beads were washed with PBS, and bound material eluted with 1.5 M NaCl. The presence of PVF1 or sGFP in the medium was monitored by western blotting with anti-PVF1 or anti-GFP, respectively.

Results

Expression of PVR

Antibodies raised against the C-terminal tail of PVR were used to determine specific sites of expression and potential activity. The antibody detects PVR as a membrane-associated protein, throughout development. In embryos the protein is prominent in tissues that showed high levels of *Pvr* RNA expression, including hemocytes and midline glial cells. In addition, expression throughout the embryonic ectoderm, beginning at stage 14, was identified (Fig. 1A-C).

The broad epithelial distribution in the embryo prompted us to examine the expression in epithelial cells at later stages of development. Indeed, in the eye imaginal disc of the third instar larvae, the receptor is also broadly expressed around the cell circumference (Fig. 1D). In the wing imaginal disc, uniform expression in the wing pouch and notum was detected. Optical cross-sections show that the receptor is present on both basolateral and apical cell surfaces in this tissue. Uniform expression in the wing continues during pupal stages (Fig. 1E-G). We focused our subsequent analysis of PVR function on the wing disc epithelium.

Expression of the ligands PVF1 and PVF3

Three putative PVR ligands have been identified following *Drosophila* genome sequencing. One of them, termed PVF1, was also identified in a functional ovary misexpression screen and shown to activate the receptor in cell culture assays. It

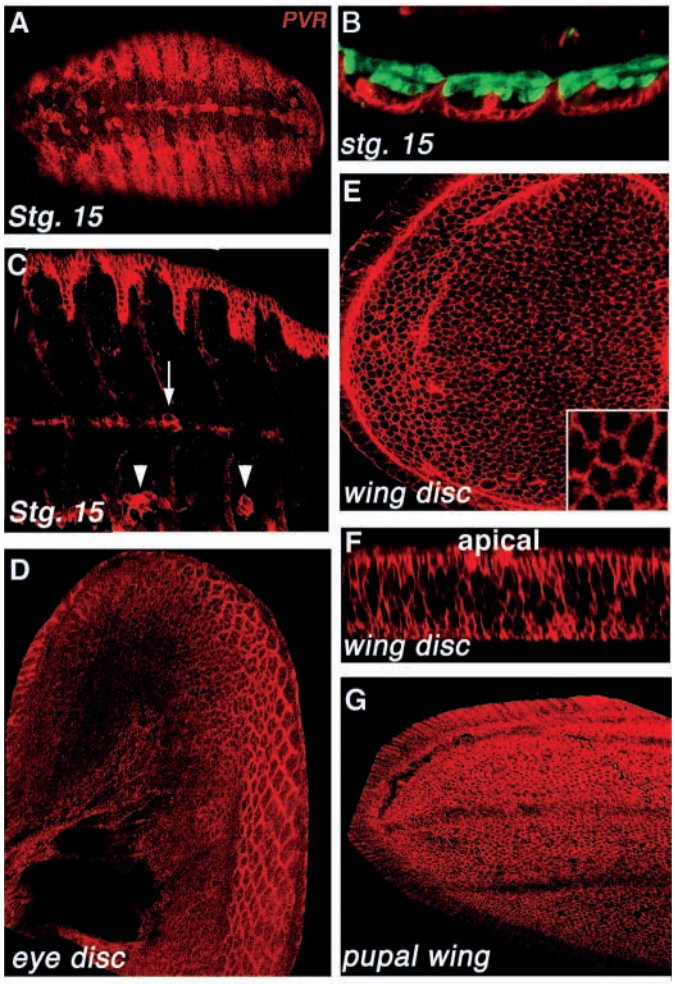

Fig. 1. Expression of PVR was detected by antibodies directed against the C-terminal region of the protein, and appeared to follow cell outlines. (A-C) From embryonic stage 14 onwards, prominent expression was detected throughout the embryonic ectoderm. PVR is also expressed in hemocytes (arrowheads) and midline glial cells (arrow). In B, muscles are stained with anti-myosin (green). (D) In the third instar larval eye disc, general cell-membrane association of PVR is observed. (E,F) In the third instar larval wing disc, the receptor is similarly expressed. F is an optical cross-section, showing the uniform distribution of PVR along the apicobasal axis. In all cross-sections, apical is shown towards the top. (G) Expression of PVR persists in the pupal wing.

represents the major PVR ligand in border cells, a migratory subset of ovarian follicle cells (Duchek et al., 2001). PVF2 was shown to be required for viability and proliferation of larval hemocytes (Munier et al., 2002). The third ligand, PVF3, has a redundant role with the other two ligands, in promoting embryonic hemocyte migration (Cho et al., 2002). We generated antibodies against PVF1 and demonstrated their capacity to recognize this protein in embryos, in a pattern similar to the one observed for the *Pvf1* transcript by RNA in situ hybridization (not shown). These antibodies do not cross react with the other two ligands, as demonstrated by their failure to detect expression of PVF2 and PVF3 in the embryonic midline. In larval wing discs, PVF1 is specifically localized to the apical side of the disc epithelium (Fig. 2A). In this domain the disc forms a sac-like structure, with the layer of squamous peripodial cells on the opposite side. The pupal wing is a bilayered structure, with the basal side of each layer facing the other, and the apical sides facing outward. PVF1 localization in the pupal wing remained apical (Fig. 2I). Antibodies were also raised against PVF3, and shown to detect the expected embryonic midline expression (not shown). In the wing disc, they detect a distinct apical distribution, similar to PVF1.

As the endogenous PVF3 was readily detected, we were able to test its segregation between intracellular and extracellular compartments. Live discs were incubated with PVF3 antibodies, and fixed only subsequently. This protocol exclusively detects the extracellular ligand (Strigini and Cohen, 2000). A prominent apical staining is found, indicating that the majority of PVF3 detected in fixed discs is extracellular (Fig. 2B).

Overexpression of PVF1, using *MS1096-Gal4*, a strong wing-specific driver, retained the apical localization of PVF1 (Fig. 2C). Despite the high levels of apical PVF1 (one to two orders of magnitude above endogenous levels), we did not detect any spread of the ligand to the basolateral side, indicating that the cell junctions form an efficient barrier to PVF1 diffusion towards the basolateral domain. Incubation of live discs overexpressing PVF1 with the antibody demonstrated that the majority of apical PVF1 is extracellular (not shown). The restricted apical localization of overexpressed PVF1 was maintained at the pupal stage (not shown).

Both endogenous PVF1 and PVF3 accumulate on the apical side of the disc epithelium. This is unusual, as other ligands used for patterning the wing disc (e.g. WG) were shown to be localized at the basolateral side (Strigini and Cohen, 2000). To ask if PVF1 and PVF3 use a common machinery for their secretion which results in apical accumulation, we overexpressed both ligands simultaneously. Overexpression of PVF1 alone did not perturb its apical accumulation. By contrast, overexpressed PVF3 was detected in a punctate pattern within the wing disc cells (Fig. 2D). The ligand failed to be secreted, probably owing to saturation of specific components of the secretory pathway, and no staining was detected when the extracellular PVF3 was probed by staining live discs (not shown). Co-expression of PVF1 with PVF3 led to a significant reduction in the level of apical PVF1, and elevated levels in punctate structures within the cells (compare Fig. 2C with 2E). In many of these puncta, colocalization of PVF1 and PVF3 was observed (Fig. 2F, inset).

The capacity of PVF3 overexpression to inhibit secretion of PVF1 is specific. When expressed alone, secreted GFP (sGFP) could be detected in both apical and basolateral domains (Fig. 2G). No alterations in this pattern were observed following co-expression with PVF3 (Fig. 2H). Optical sections show that sGFP was located between the cells in the basolateral region, while PVF3 was trapped within the cells (Fig. 2H, inset). These results indicate that PVF1 and PVF3 use a discrete secretory mechanism, leading to exclusive apical deposition, which is distinct from the bulk flow, represented by sGFP.

We next examined whether PVF1 is sequestered following secretion, or free to diffuse within the apical domain. As overexpressed PVF1 maintained its restricted apical localization, we expressed the ligand in clones of cells marked

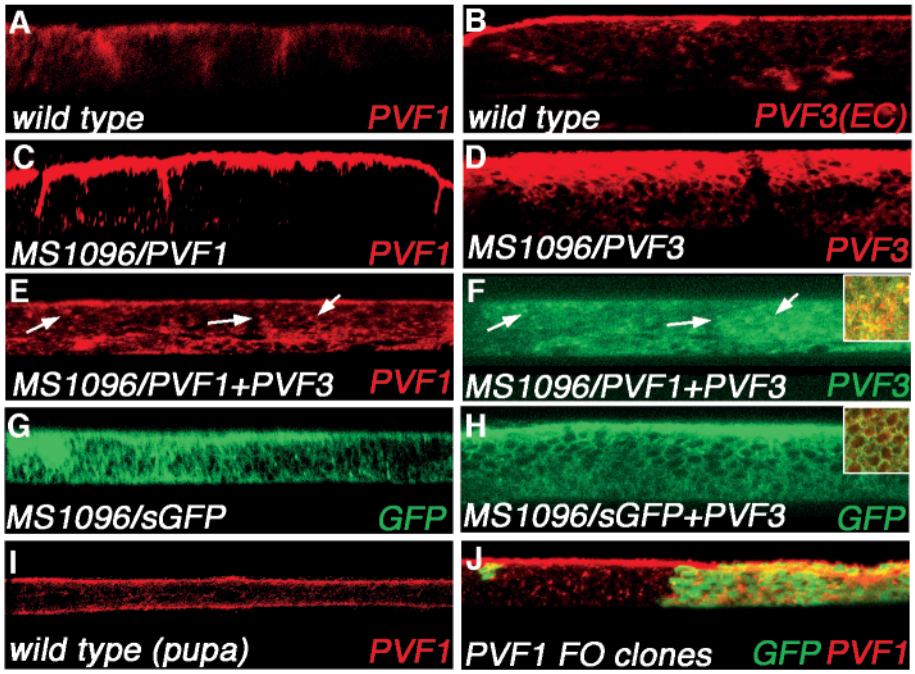

Fig. 2. Apical localization of PVF1 and PVF3. All panels except insets represent optical cross-sections of third instar larval wing imaginal discs. (I) A section of a pupal wing. Apical is towards the top, and basal towards the bottom. (A) Apical accumulation of endogenous PVF1 in a wild-type wing imaginal disc. (B) Similarly, PVF3 is also apically concentrated. In this panel, live discs were incubated with the PVF3 antibody prior to fixation, thus detecting only the extracellular PVF3. (C) Upon overexpression by *MS1096-Gal4*, PVF1 maintains its apical localization, whereas PVF3 accumulates within the producing cells (D). (E,F) Overexpression of PVF1 together with PVF3 reduced the portion of apically localized PVF1, which instead accumulated within the cells. In many of the intracellular puncta, colocalization of PVF1 and PVF3 was observed (arrows). The inset shows a section from the basolateral region. (G) Discs expressing sGFP show concentration on the apical side, but after secretion, significant levels were also detected between the cells on the basolateral region. (H) Co-expression of sGFP with PVF3 did not alter its distribution. The inset is a section obtained from the basolateral region. Comparison with the inset in F demonstrates that while PVF1 is trapped within the cells, sGFP is readily detected between the cells. (I) In a wild-type bilayered pupal wing, accumulation of PVF1 on the apical side of both layers is observed. (J) Clones overexpressing PVF1 (marked by GFP) were generated. PVF1 localization was monitored at a laser intensity that detects the overexpressed protein but not the endogenous one. Apical accumulation of PVF1, which was uniform above expressing and non-expressing cells was observed.

by GFP (‘flipout’ clones), and monitored its distribution over adjacent cells. Detection was performed under conditions of low laser illumination intensity, which identify only overexpressed PVF1 but not the endogenous ligand. Excess PVF1 could be uniformly detected within the entire apical space of the disc epithelium (Fig. 2J). This result indicates that following apical secretion of PVF1, the ligand is not trapped on the apical extracellular surface of the producing cells, but is capable of extensive lateral diffusion.

Heparin binding properties of PVF1

One of the hallmarks of vertebrate VEGF molecules is their capacity to bind heparin. This property is mapped to a distinct domain located C-terminal to the receptor-binding domain. Removal of this domain in one of the mammalian VEGF splice isoforms ($VEGF^{121}$), generates a molecule that is capable of binding the receptor, while failing to bind heparin (Park et al., 1993a). Although PVF1 shows no distinct homology to the heparin-binding domain of VEGF, it may still have the capacity to bind heparin. To test for heparin-binding properties of PVF1, medium derived from Schneider S2 cells overexpressing PVF1 was collected. Incubation with heparin-Sepharose beads showed a specific and efficient binding of PVF1. Most of the protein was removed from the medium. The bound PVF1 was eluted from the beads at 1.5 M NaCl. No such heparin binding was detected for the control secreted GFP protein (Fig. 3).

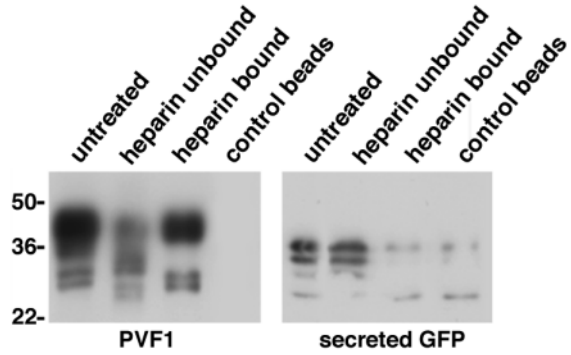

Fig. 3. PVF1 binds heparin. The capacity of PVF1 to bind heparin was examined as a possible mechanism for activation of the ligand in the wing imaginal disc. Schneider S2 cells were transfected with a PVF1-expression construct, and medium was collected. Incubation of this medium with heparin beads showed that most of the PVF1 protein was removed by the beads, and could be efficiently eluted by 1.5 M NaCl. PVF1 did not bind to control sepharose beads. By contrast, medium of cells expressing secreted GFP showed that the protein was not bound to the heparin beads. Equal amounts of medium were loaded before and after incubation with the beads. PVF1 was detected by probing the blot with anti-PVF1 serum, and sGFP was followed with anti-GFP.

PVR loss of function in the wing imaginal disc

A loss-of-function allele of *Pvr* was previously described (Cho et al., 2002). To asses the possible requirements for PVR during wing disc development, we used this allele to generate *Pvr*-mutant clones in the wing disc. The size of the clones was comparable with that of wild-type twin clones (Fig. 4A). Epithelial cells of the wing imaginal disc are elongated and form

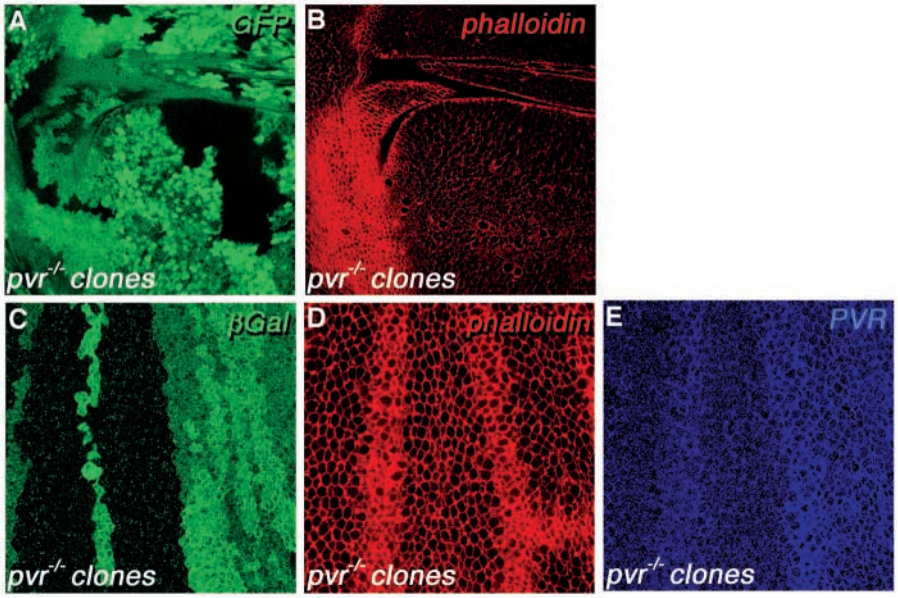

Fig. 4. Clones lacking endogenous PVR have no apparent wing phenotype. (A,B) Clones homozygous for a *Pvr* mutation (marked by absence of GFP) show normal tissue organization and F-actin distribution in the larval wing imaginal disc. Note that the size of the mutant clones is similar to that of the wild-type twin clones showing enhanced levels of GFP. As the disc is slightly tilted, this optical section shows the apical domain of the disc on the left part, and the basolateral region on the right. (B) Note that normal F-actin accumulation is observed in the former, and no ectopic accumulation in the latter, regardless of the clone boundaries. (C-E) Similar *Pvr* mutant clones were analyzed in the pupal wing, marked by the absence of β-gal staining, or PVR staining. In the case of PVR staining, only a background signal that is not membrane-associated was detected within the clones, implying that the PVR protein expressed by this allele does not contain the C-terminal domain recognized by the antibody. Again, normal tissue organization and F-actin distribution was observed.

a continuous, highly polarized single-layered epithelium, characterized by apical localization of F-actin belts, at the adherens junctions. Proteins like Discs large (DLG) are localized at the septate junctions, which are positioned below the adherens junctions (Watson et al., 1994). No phenotype was identified in *Pvr*-mutant clones in terms of the epithelial organization of the tissue, or the polarity of the cells as monitored by apical localization of F-actin (Fig. 4B) and DLG (not shown). When clones were analyzed in the pupal wing, again no phenotypes could be detected using the same criteria (Fig. 4C-E).

Similarly, expression of *UAS-Pvr RNAi* constructs in wing discs using either *MS1096-Gal4* or the spatially restricted driver *ptc-Gal4*, reduced the level of PVR (see Fig. 7A), but did not result in any phenotypes (not shown).

Uniform PVR activation induces tumorous growth

In view of the possibility of a redundant function for PVR in the wing, we sought to gain insights into the normal function through misexpression experiments. This is especially pertinent as the apical localization of the ligands may imply a spatial control of PVR activation. To examine the possible importance of polarized PVR activation, we expressed a constitutively dimerizing PVR construct, where the extracellular region was replaced by the lambda dimerization domain (λPVR). This construct was previously shown to be potent in the follicular epithelium (Duchek et al., 2001). Expression of *UAS-λPvr* induced by *MS1096-Gal4* gave rise to a dramatic phenotype, which was completely penetrant even when the induction levels were compromised at 18°C. Most larvae continued to grow in size beyond the third instar and failed to pupariate. The wing discs of these larvae were several times larger than wild-type discs, and appeared completely disorganized. Sections of the proliferating discs showed multiple layers missing all aspects of polarity (Fig. 5A-E). Similar giant larvae and tumorous disc phenotypes have been described for loss-of function mutants in *dlg*, *scribble* and *l(2)gl* (Watson et al., 1994). In these mutants, imaginal discs lost apicobasal polarity, and continued proliferating as unorganized, multilayered structures. Consequently the larvae grew in size, and pupariation was not initiated.The level of F-actin within the λPVR-expressing cells was markedly elevated. In addition, instead of forming regular ring structures, microfilaments appeared disorganized. Finally, the apical restriction of F-actin was abolished, and a uniform distribution around the cell circumference was observed (Fig. 5G,H). EM examination of these cells revealed multiple adherens junctions instead of the typical single apical adherens junction per cell (Fig. 5I,J).

Staining of the DLG protein showed a uniform distribution around the cell circumference (Fig. 5K), suggesting that in discs expressing λPVR septate junctions are intact, although not correctly polarized. Localization of a second marker, LGL, allowed us to verify this interpretation. LGL is a protein that exists in a soluble, cytoplasmic form and an insoluble form thought to be associated with membranes and the actin cytoskeleton (Strand et al., 1994). Association of LGL with the membrane requires intact septate junctions, because in *dlg* or *scribble* mutants, LGL is found only in the cytoplasm (Bilder et al., 2000). In λPVR-expressing cells, LGL retained its membrane association, possibly to even higher levels than normal (Fig. 5L-N). These observations demonstrate that septate junction components are retained in the membrane of λPVR cells, and furthermore, they maintain at least some of their roles.

Overexpression of PVR induces actin microfilament polymerization

The dramatic effect of λ-PVR expression prompted us to study the phenotypic consequences resulting from overexpression of PVR. Ubiquitous expression of a full-length construct of PVR in the wing disc results in pupal lethality. When we analyzed the wing disc upon overexpression of PVR in a specific domain

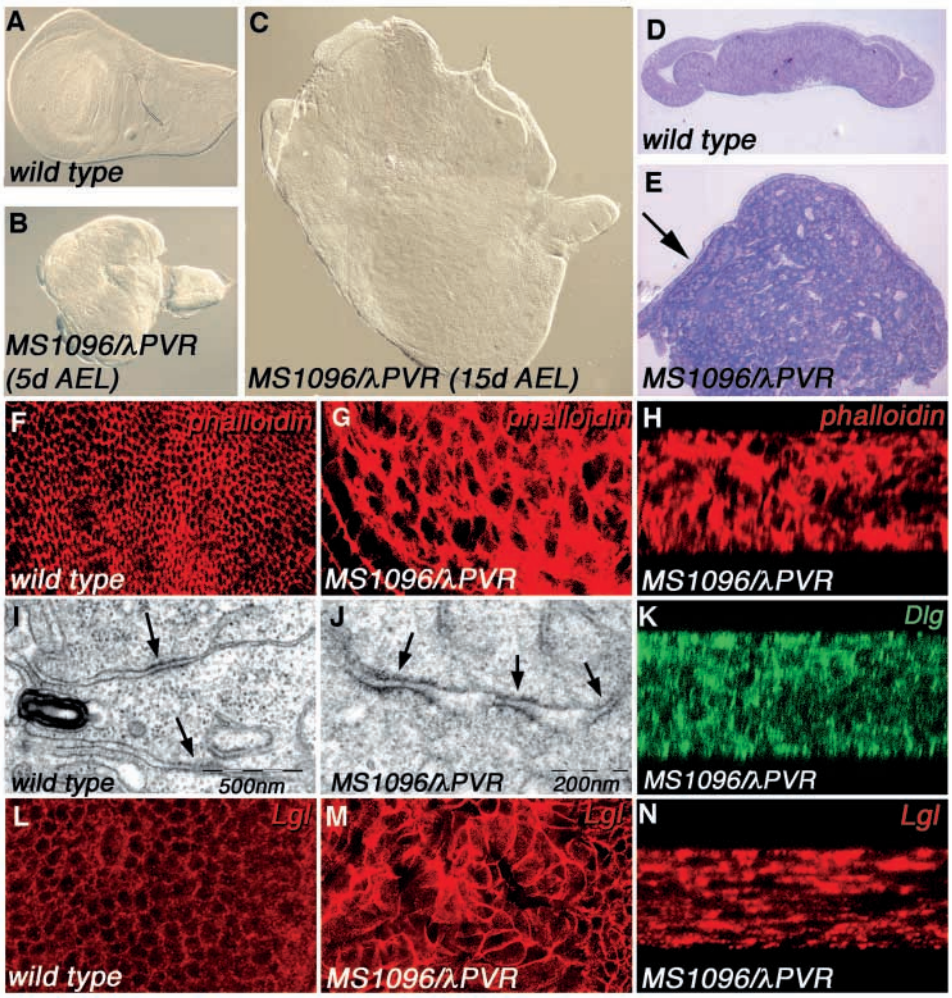

Fig. 5. Uniform PVR activation abolishes cell polarity and generates tumorous wing discs. (A-C) A constitutively activated λPVR construct was expressed in the wing imaginal disc, to follow the consequences of uniform PVR activation. Five days after egg lay (AEL), the size of these discs was normal, but aberrant overall tissue organization was observed (compare a wild-type disc in A with B). These larvae failed to pupariate and continued to grow. Fifteen days AEL, these larvae contained wing imaginal discs that were approximately five times larger than normal discs (C). (D,E) Cross-sections show that discs expressing λPVR (E) were multilayered, and the cells appeared non-polarized, in contrast to the layered epithelium of a wild-type disc (D). The arrow in E shows a region at the periphery of the disc where *MS1096-Gal4* is not expressed, and the simple epithelial structure was retained. (F) Apical section through a wild-type disc shows the ordered organization of F-actin. (G) In *MS1096-Gal4*/*UAS*-λPVR discs a higher level of F-actin with a highly unorganized distribution is observed. (H) Optical cross-section of this disc shows that within the multilayered structure that is generated, F-actin appears to be distributed in a uniform, non polarized manner within each cell. (I,J) The above observation is corroborated by EM studies. While wild-type disc cells show only a single adherens junction per cell (marked by electron-dense material on both sides of the membrane bilayer, arrows), multiple adherens junctions per cell were identified in the cells expressing λPVR. (K) The presence of DLG associated with the membranes of λPVR cells suggests that the septate junctions are retained. However, their distribution is no longer polarized. (L) In wild-type epithelial cells, LGL is associated with the plasma membrane. (M,N) In λPVR discs, LGL continues to be associated with the membrane (possibly even at higher levels), indicating that the septate junctions that mediate its membrane association are functional. Taken together, these results imply that normal activation of PVR in the wing imaginal disc is polarized, as uniform PVR activation leads to a complete loss of cell polarity. In addition to the disrupted distribution of polarity markers, λPVR specifically elevates the levels of F-actin.

along the anteroposterior border using the *dpp-Gal4* driver, we noticed a significant elevation in the level of F-actin along the basolateral area of the epithelium (Fig. 6B,C). Conversely, the levels of G-actin were slightly lower than in the surrounding cells (Fig. 6D) indicating that the elevation in PVR levels enhanced actin polymerization, rather than induced actin transcription. The elevation in actin polymerization was accompanied by elevation in the Chickadee (Profilin) protein that binds actin monomers (Fig. 6F). Consequently, an irregular fold was formed within the domain expressing PVR (Fig. 6H).

As PVR overexpression was lethal, we looked for a way to express the native protein in lower amounts. While analyzing PVR expression in the different lines expressing *Pvr-RNAi*, we noted one instance in which the levels of PVR in the domain expressing ds-RNA were slightly higher than normal, by approximately twofold (Fig. 7B). We termed this line RNAi-gain of function (*RNAi-GOF*). The insertion of the UAS construct in *RNAi-GOF* is in cytogenetic band 27A1-27A2, 1.5 Mb from the endogenous *Pvr* gene (28F3-28F5). Although the insertion is not in very close proximity, it still raises the possibility of cis-interaction between the loci, upon binding of the Gal4 transcriptional activator, thus accounting for the unexpected rise in PVR levels. In contrast to the other RNAi lines in which PVR levels were reduced (Fig. 7A) that gave no wing phenotype, induction of RNAi-GOF by MS1096-Gal4 resulted in wing blisters (Fig. 7I,J).

We analyzed wing discs that expressed *RNAi-GOF* under the control of *ptc-Gal4*. In accordance with the phenotypes caused by *UAS-Pvr* expression, F-actin organization was altered specifically at the basal side of the epithelium (Fig. 7C). Elevation in Chickadee levels was also observed (not shown). Examination of components of the adherens junction (phospho-tyrosine) as well as septate junctions (DLG protein) revealed no change in the localization or the levels of these proteins (not shown).

We also examined the effects of expressing *RNAi-GOF* in the pupal wing, to determine the basis for the adult blistering

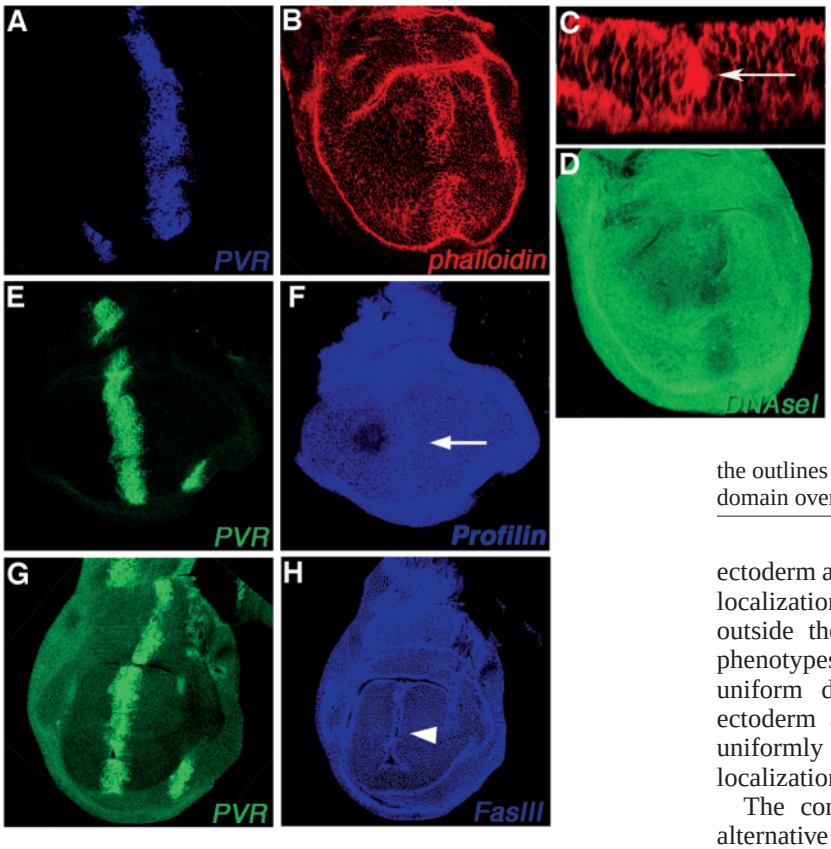

Fig. 6. PVR overexpression induces actin polymerization. *UAS-Pvr* was overexpressed in the wing disc by the *dpp-Gal4* driver (A,D,F). Elevation in actin microfilaments was observed in cells overexpressing PVR as monitored by Phalloidin staining (B). Cross-section shows that the excess actin filaments are located in the basolateral area of the cells (C, arrow). Conversely, a reduction in actin monomers was observed in the same region by staining with flourescein-DNaseI (D). Profilin (Chickadee), which binds free actin and affects actin polymerization dynamics, is elevated in the stripe of PVR overexpression (F, arrow). The changes in actin cytoskeleton following PVR overexpression are eventually manifested in a general change in epithelial morphology. An extra and irregular fold is observed and demonstrated with FasIII which marks the outlines of all epithelial cells (H, arrowhead). E and G show the domain overexpressing PVR.

phenotype. In the pupal wing, F-actin in each layer is normally enriched not only at the apical side as in larval discs, but also in the basal region (Fig. 7D,F). Although the organization of apical F-actin was unaffected, an ectopic and highly irregular accumulation of F-actin at the basolateral side of *MS1096Gal4/RNAi-GOF* pupal wings was observed (Fig. 7E,G).

The specificity of the gain-of-function effect was strengthened by genetic interaction experiments. Females heterozygous for the driver *MS1096-Gal4* and *RNAi-GOF* show a mild wing phenotype (Fig. 7I). When the ligand *PVF1* was overexpressed, accumulation of excess ligand at the apical side was observed (Fig. 2C), but no apparent phenotype ensued (Fig. 7K). If expression of the *RNAi-GOF* construct leads to a gain-of-function phenotype, excess apical PVF1 should result in a more severe phenotype. Indeed, co-expression of *RNAi-GOF* with *Pvf1* gave rise to an enhanced wing phenotype that was fully penetrant. Females containing a single copy each of *MS1096-Gal4*, *UAS-RNAi-GOF* and *UAS-Pvf1* showed a dramatic enhancement. The wings were not only blistered, but also reduced in size and highly folded (compare Fig. 7L with 7I,K). Thus, the excess apical PVF1 enhanced the effect of RNAi-GOF.

PVF localization and PVR activation phenotypes are tissue specific

In view of the retention of PVF1 and PVF3 on the apical extracellular surface of the wing imaginal disc, we examined whether a similar localization also takes place in other epithelial tissues. PVF1 was overexpressed in the embryonic ectoderm and the eye imaginal disc. In both cases, no polarized localization of the ligand could be observed either within or outside the cells (Fig. 8A,B). Furthermore, no deleterious phenotypes resulted from this manipulation (Fig. 8A). As the uniform distribution of ectopic PVF1 in the embryonic ectoderm and eye disc is expected to trigger the receptor uniformly in the responding cells we concluded that apical localization of PVF1 in these tissues is not necessary.

The constitutively dimerizing form, λPVR, provides an alternative method to activate the receptor uniformly. We expressed λPVR in embryonic tissues and other larval imaginal discs. No defects were observed in polarized embryonic epithelia (e.g. ectoderm or trachea). Although expression of λPVR results in embryonic lethality, cuticular defects appear to be restricted to holes at the termini, without any overall abnormalities (Fig. 8C). Similarly, in the eye disc, no apparent abnormalities in tissue organization or F-actin distribution were observed following λPVR expression (Fig. 8D,E). These results imply the presence of specific components in the wing disc, which may transmit or facilitate the intracellular responses to polarized activation of PVR, only in tissues where the ligand is apically restricted.

Discussion

This work examined the involvement of PVR and its ligands in the maintenance of epithelial cell polarity in the wing imaginal disc. Although the receptor is broadly distributed, the ligands are apically restricted, and could lead to polarized receptor activation. Phenotypes resulting from PVR gain-of-function circumstances imply that apically polarized PVR activation is normally essential for regulated polymerization and bundling of actin microfilaments.

Expression of PVR and its ligands

Examination of PVR protein revealed a broad expression in epithelial tissues in the embryo from stage 14, and in the imaginal discs. PVR expression is not confined along the apicobasal axis of the cells. In contrast to the uniform distribution of the receptor, there is restricted apical localization of the ligands PVF1 and PVF3 within the wing disc epithelium.

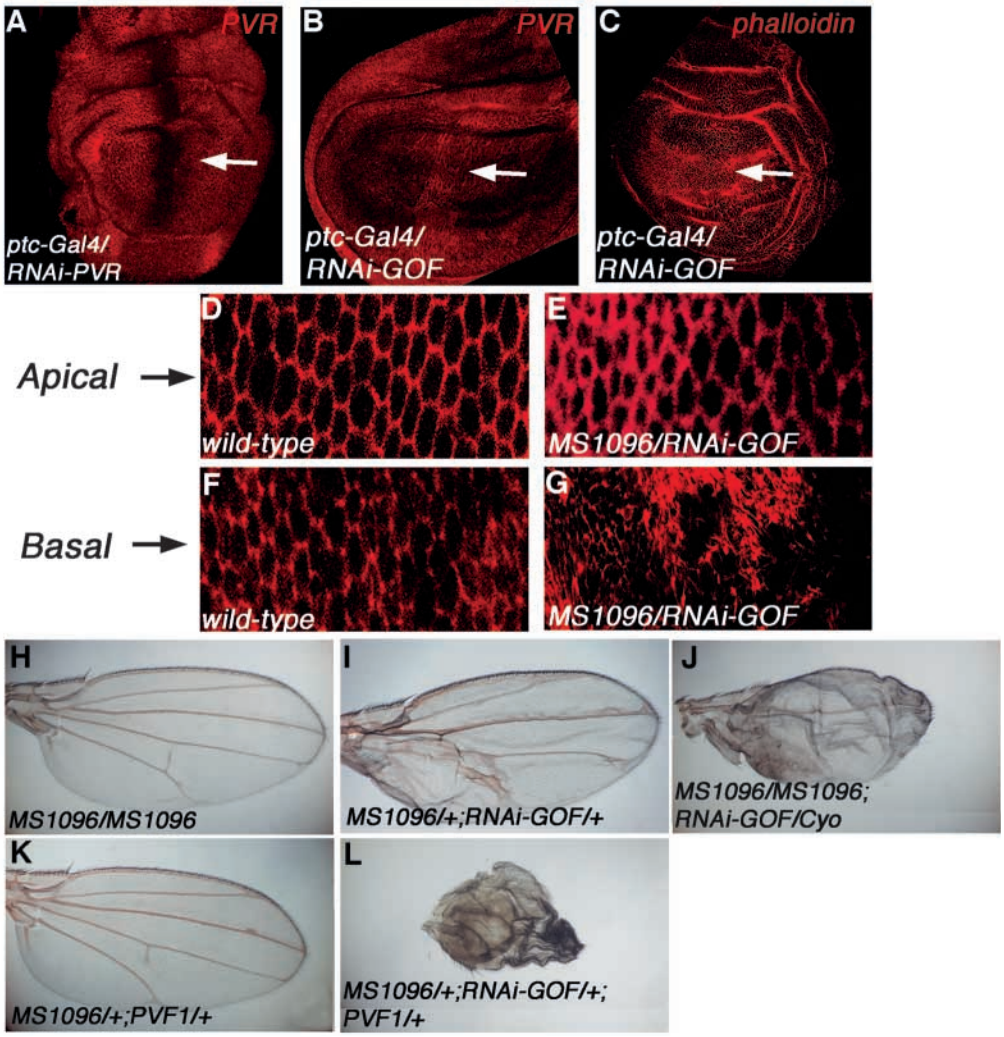

Fig. 7. Synergistic interaction between elevated PVR levels and excess apical PVF1. As PVR overexpression leads to pupal lethality, we were able to induce lower levels of PVR by using an unusual insertion of the *UAS-Pvr-RNAi* construct. Although most *Pvr-RNAi* constructs lead to a reduced level of PVR (A, arrow), this insertion (termed *RNAi-GOF*) gave rise to elevated PVR levels (B, arrow). This elevation is also reflected in defects in actin microfilament organization at the basal side of the epithelium (C, arrow). As *RNAi-GOF* flies were viable, it was possible to examine their pupal wings. We noted that whereas the organization of apical F-actin was unaltered (D,E), a dramatic misorganization was induced at the basal domain (F,G). Expression of adult wing phenotype. Females carrying two copies of *MS1096-Gal4* had normal wings (H). Minor defects could be observed with a single dose of *MS1096-Gal4* and *UAS-RNAi-GOF* (I). This phenotype was enhanced when having two copies of the Gal4 driver (J). Overexpression of *Pvf1*, which accumulates at the extracellular apical side, does not lead to defects in the wing (K). Flies containing a single dose of the driver and *UAS-RNAi-GOF* and *UAS-Pvf1* show a dramatic enhancement of the phenotype (L). This demonstrates that the phenotypes observed following PVR overexpression represent activation of the endogenous pathway by its ligands.

The mechanism responsible for the apical accumulation of PVF1 and PVF3 in the wing disc is intriguing. As cell junctions are likely to form barriers that can not be bypassed by exogenous ligand, apical accumulation may imply preferential secretion of PVR ligands at the apical compartment. It is possible that PVF1 and PVF3 are targeted to vesicles that are specifically marked for secretion at the apical surface. The observation that PVF3 overexpression compromises the secretion of PVF1 but not that of sGFP, supports such a possibility. The presence of distinct secretory vesicles which are targeted to apical versus basolateral compartments has been previously observed (Jacob and Naim, 2001).

What further interactions do PVF1 and PVF3 undergo, once secreted to the apical extracellular compartment? One possible interaction involves binding to heparan-sulfate proteoglycans on the cell surface. The vertebrate VEGF proteins have a defined heparin-binding domain at the C terminus that is distinct from the receptor-binding moiety (Park et al., 1993b). The equivalent C-terminal domain of PVF1 does not show a distinct homology to the heparin-binding domain of VEGF. We have shown, however, that PVF1 secreted by S2 cells can bind heparin beads. To examine if PVF1 is trapped on the cell surface following secretion, we created marked clones of cells overexpressing PVF1. We find that the ligand is uniformly redistributed along the entire apical surface, including the surface of cells not secreting the ligand. Although the ligand is capable of spreading readily within the apical plane, it is incapable of crossing the cell junctions, and is thus excluded from the basolateral extracellular compartment.

What is the role of PVR in the wing disc?

Accumulation of PVF1 and PVF3 at the extracellular apical compartment implies that the PVR receptor is activated in a polarized fashion. Does such an apically polarized pattern of activation play a role in shaping the wing disc epithelium? The most direct way to examine PVR function in the wing disc is to generate clones for null *Pvr* alleles, and follow their phenotype. The *Pvr*-mutant clones were similar in size to their wild-type twins, and within the clones no aberrant morphology or misorganization of actin was detected. We thus conclude that PVR has a redundant role in the wing. Nevertheless, a series of dramatic wing phenotypes is induced following

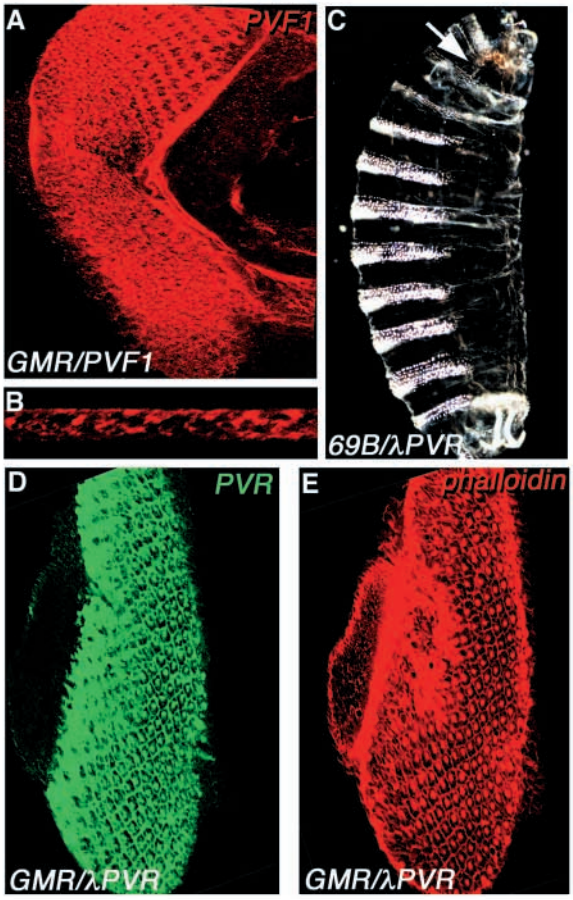

Fig. 8. Polarized activity of PVF1/PVR is specific to the wing imaginal disc. The polarizing activity of PVF1/PVR was followed in other epithelial tissues in which PVR is normally expressed. (A,B) In the eye imaginal disc, induction of *Pvf1* by *GMR-Gal4* leads to a uniform apicobasal distribution of PVF1, without any apparent defects. (C) Uniform ectodermal expression of *λPvr* in the embryo (by *69B-Gal4*) did not disrupt the polarity of the ectoderm and the secreted cuticle. Arrow shows the position of a hole induced in the dorsal head region. (D,E) Uniform expression of *λPvr* in the eye disc did not disturb the organization of the epithelium and the distribution of actin. Taken together, these results demonstrate that the apical retention of PVF1, as well as the responses to λPVR, are specific to the wing imaginal disc.

expression of various PVR constructs. Our analysis leads us to propose that these phenotypes represent gain-of-function circumstances following inappropriate activation of PVR on the basolateral side of the wing disc epithelium.

We were first drawn to this interpretation by the dramatic effects of non-restricted and constitutive receptor activation, achieved by expression of λPVR in the wing disc epithelium. The epithelium lost its polarity, multiple cell layers were generated, and giant tumorous discs were formed. Ectopic accumulation of F-actin around the circumference of the cells was observed, and corroborated by the identification of multiple adherens junctions in EM images.

The phenotype created by expressing λPVR in the wing disc is reminiscent of the phenotype described for loss of the septate junction proteins DLG and Scribbled, as well the LGL protein. We believe that the alterations in cell polarity following λPVR expression are less severe than the *dlg*, *scribble* or *lgl* mutant phenotypes. Although excess adherens junctions are established and the septate junctions are mislocalized, the LGL protein, which requires intact septate junctions for its insertion into the membrane, is found associated with the membrane in wing discs expressing λPVR. The tumorous growth of the cells is believed to be a secondary consequence of the loss of polarity, which may lead to impairment of cell-cell communication.

We examined also the consequences of misexpressing full-length PVR. We noticed significantly higher levels of F-actin in the basolateral area of the cells expressing PVR, while the level of actin monomers was lower. This indicates that PVR has a localized effect on actin polymerization, rather than a general role in actin monomer synthesis. We also noticed elevation in Profilin (chickadee) protein levels. Profilin binds actin monomers in a way that inhibits nucleation and elongation of pointed ends but promotes rapid elongation of uncapped barbed ends, leading to depletion of the actin monomer pool (Amann and Pollard, 2000).

Overexpression of the ligands alone did not lead to any phenotype, while even mild overexpression of the receptor resulted in pronounced phenotypes. Moreover, these phenotypes were strongly enhanced by elevating the levels of PVF1 in the apical domain. There are two possible explanations for the overexpression phenotype. The overall levels of receptor activation may be important. The receptor could be present in limited amounts, so that increasing its levels allows more ligand at the apical side to bind and activate receptors. Alternatively, polarized activation of the receptor that normally takes place is disturbed, because of redistribution of the ligand. This may happen by recycling of the ligand-bound receptor inside the cells. The fact that elevation in PVR levels resulted in basolateral polymerization of actin, while the ligand is normally found on the apical side supports this possibility. Mislocalized activation of the receptor may also take place because of spontaneous dimerization caused by the higher levels of the receptor.

It is interesting to note that while λPVR gave rise to a dramatic phenotype when expressed in the wing disc or the follicular epithelium, no apparent phenotypes were observed following expression in the embryonic ectoderm or the eye disc. Some of the intracellular elements that may be essential for relaying the signals resulting from PVR activation could thus be expressed or active only in a restricted set of tissues.

In the embryonic ectoderm and eye disc where λPVR was inactive, we also failed to see apical accumulation of PVF1. The correlation between the capacity of the wing epithelium to localize the ligands apically, on the one hand, and to respond to uniform PVR activation, on the other, strengthens the notion that apical activation of PVR is instructive in this tissue.

What can the ectopic phenotypes teach us with regards to the normal downstream responses to PVR activation in the wing epithelium? The primary defect upon overexpression of PVR is misorganization of the actin cytoskeleton at the basolateral side. In addition, expression of the constitutively active receptor results in multiple adherens junctions. We thus suggest that apically restricted PVR activation provides signals that facilitate the formation of F-actin at the adherens junctions. This role is reminiscent of the activity of PVR in the border cells of the ovary, where polarized activation by PVF1,

expressed in the oocyte, participates in guiding the migration of the border cells (Duchek et al., 2001). It is tempting to suggest that polarized PVR activation regulates migration or cell polarity, using a common set of intracellular responses leading to localized actin polymerization.

We thank Ayelet Schlesinger for providing the sGFP flies, Limor Landsman for the initial PVR disc stainings, Ilana Sabanay for EM preparations and Ruth Tal for technical help. We also thank P. Bryant, F. Matzuzaki, P. Rorth, the Berkeley *Drosophila* Genome Project, Exelixis, the Developmental Studies Hybridoma Bank, and the Bloomington stock center for antibodies, cDNAs and fly strains. We are grateful to D. Bilder, R. Fehon, P. Rorth and E. Zelzer for fruitful discussions. This work was funded by grants from the Israel Science Foundation, the Minerva Foundation and the Forchheimer Center to B.S., who is an incumbent of the Hilda and Cecil Lewis professorial chair in Molecular Genetics.

References

Amann, K. J. and Pollard, T. D. (2000). Cellular regulation of actin network assembly. *Curr. Biol.* **10**, R728-R730.

Bilder, D. (2001). PDZ proteins and polarity: functions from the fly. *Trends Genet.* **17**, 511-519.

Bilder, D., Li, M. and Perrimon, N. (2000). Cooperative regulation of cell polarity and growth by Drosophila tumor suppressors. *Science* **289**, 113-116.

Borrmann, C. M., Mertens, C., Schmidt, A., Langbein, L., Kuhn, C. and Franke, W. W. (2000). Molecular diversity of plaques of epithelial-adhering junctions. *Ann. New York Acad. Sci.* **915**, 144-150.

Braga, V. M. (2002). Cell-cell adhesion and signalling. *Curr. Opin. Cell Biol.* **14**, 546-556.

Cho, N. K., Keyes, L., Johnson, E., Heller, J., Ryner, L., Karim, F. and Krasnow, M. A. (2002). Developmental control of blood cell migration by the Drosophila VEGF pathway. *Cell* **108**, 865-876.

Drubin, D. G. and Nelson, W. J. (1996). Origins of cell polarity. *Cell* **84**, 335-344.

Duchek, P., Somogyi, K., Jekely, G., Beccari, S. and Rorth, P. (2001). Guidance of cell migration by the Drosophila PDGF/VEGF receptor. *Cell* **107**, 17-26.

Fristrom, D., Gotwals, P., Eaton, S., Kornberg, T. B., Sturtevant, M., Bier, E. and Fristrom, J. W. (1994). Blistered: a gene required for vein/intervein formation in wings of Drosophila. *Development* **120**, 2661-2671.

Jacob, R. and Naim, H. Y. (2001). Apical membrane proteins are transported in distinct vesicular carriers. *Curr. Biol.* **11**, 1444-1450.

Mostov, K. E. and Cardone, M. H. (1995). Regulation of protein traffic in polarized epithelial cells. *BioEssays* **17**, 129-138.

Muller, H. A. (2000). Genetic control of epithelial cell polarity: lessons from Drosophila. *Dev. Dyn.* **218**, 52-67.

Munier, A. I., Doucet, D., Perrodou, E., Zachary, D., Meister, M., Hoffmann, J. A., Janeway, C. A., Jr and Lagueux, M. (2002). PVF2, a PDGF/VEGF-like growth factor, induces hemocyte proliferation in Drosophila larvae. *EMBO Rep.* **3**, 1195-1200.

Nagafuchi, A. (2001). Molecular architecture of adherens junctions. *Curr. Opin. Cell Biol.* **13**, 600-603.

Neumann, C. J. and Cohen, S. M. (1997). Long-range action of Wingless organizes the dorso-ventral axis of the *Drosophila* wing. *Development* **124**, 871-880.

Park, J. E., Keller, G. A. and Ferrara, N. (1993a). The vascular endothelial growth factor (VEGF) isoforms: differential deposition into the subepithelial extracellular matrix and bioactivity of extracellular matrix-bound VEGF. *Mol. Biol. Cell* **4**, 1317-1326.

Park, J. E., Keller, G. A. and Ferrara, N. (1993b). The vascular endothelial growth factor (VEGF) isoforms: differential deposition into the subepithelial extracellular matrix and bioactivity of extracellular matrix-bound VEGF. *Mol. Biol. Cell* **4**, 1317-1326.

Simons, K. and Ikonen, E. (1997). Functional rafts in cell membranes. *Nature* **387**, 569-572.

Strand, D., Jakobs, R., Merdes, G., Neumann, B., Kalmes, A., Heid, H. W., Husmann, I. and Mechler, B. M. (1994). The Drosophila lethal(2)giant larvae tumor suppressor protein forms homo-oligomers and is associated with nonmuscle myosin II heavy chain. *J. Cell Biol.* **127**, 1361-1373.

Strigini, M. and Cohen, S. M. (2000). Wingless gradient formation in the Drosophila wing. *Curr. Biol.* **10**, 293-300.

Tepass, U. (2002). Adherens junctions: new insight into assembly, modulation and function. *BioEssays* **24**, 690-695.

Tepass, U., Tanentzapf, G., Ward, R. and Fehon, R. (2001). Epithelial cell polarity and cell junctions in Drosophila. *Annu. Rev. Genet.* **35**, 747-784.

Wandinger-Ness, A., Bennett, M. K., Antony, C. and Simons, K. (1990). Distinct transport vesicles mediate the delivery of plasma membrane proteins to the apical and basolateral domains of MDCK cells. *J. Cell Biol.* **111**, 987-1000.

Watson, K. L., Justice, R. W. and Bryant, P. J. (1994). Drosophila in cancer research: the first fifty tumor suppressor genes. *J. Cell Sci. Supplement* **18**, 19-33.